TECHNICAL RESEARCH REPORT

Real-Time Growth Rate Metrology for a Tungsten CVD Process by Acoustic Sensing

by L. Henn-Lecordier, John N. Kidder, Jr., Gary W. Rubloff, C. A. Gogol, A. Wajid

T.R. 2000-24

Real -Time Growth Rate Metrology for a Tungsten CVD Process by Acoustic Sensing

L. Henn-Lecordier, J.N. Kidder, Jr., G.W. Rubloff
Department of Materials and Nuclear Engineering and Institute for Systems Research
University of Maryland, College Park, MD 20742

C. A. Gogol, A. Wajid
Inficon, Inc.
East Syracuse, NY 13057

ABSTRACT

An acoustic sensor, the Leybold Inficon Composer™, was implemented downstream to a production-scale tungsten chemical vapor deposition (CVD) cluster tool for in-situ process sensing. Process gases were sampled at the outlet of the reactor chamber and compressed with a turbo-molecular pump and mechanical pump from the sub-Torr process pressure regime to above 50 Torr as required for gas sound velocity measurements in the acoustic cavity. The high molecular weight gas WF_6 mixed with H_2 provides a substantial molecular weight contrast so that the acoustic sensing method appears especially sensitive to WF_6 concentration. By monitoring the resonant frequency of exhaust process gases, the depletion of WF_6 resulting from the reduction by H_2 was readily observed in the 0.5 Torr process for wafer temperatures ranging from 300 to 350 C. Despite WF_6 depletion rates as low as 3-5%, in-situ wafer-state metrology was achieved with an error less than 6% over 17 processed wafers. This in-situ metrology capability combined with accurate sensor response modeling suggests an effective approach for acoustic process sensing in order to achieve run-to-run process control of the deposited tungsten film thickness.

INTRODUCTION

Chemical sensing techniques for monitoring and controlling chemical vapor deposition (CVD) processes have become increasingly important. In semiconductor manufacturing, the development of diagnostics for in-situ, real-time monitoring and control is driven by the need for improvements in production efficiency through the use of process control including both real-time detection of process drift and equipment failure. As wafer size increases, the cost of process evaluation via test wafers and the product losses associated with process drift and/or equipment failure motivate the use of advanced sensors for monitoring and control in IC manufacturing.[1,2]

Gas phase chemical sensing provides information on the extent of reactions in processes such as chemical vapor deposition (CVD) and is critical to achieve wafer-state metrology for in-situ process control. Prior approaches have especially focused on sensors that detect concentrations of individual gas-phase species, such as FT-IR spectroscopy [3-8], UV spectroscopy [9-11], and mass spectrometry.[12-16] In-situ growth rate

metrology by detection of the gas-phase composition downstream of the wafer by mass spectrometry has been reported for silicon and tungsten CVD.[13-15] For the case of tungsten CVD, accurate wafer-state characterization by mass-spectrometry is limited by the high reactivity of the WF_6/H_2 reagents that generates process drifts and high background levels from chemical reactions on the wall surface and in the ionizer. [15]

Acoustic sensors can be used to monitor the depletion of reagents and/or generation of products by measuring in an acoustic cavity the speed of sound of the exhaust gas mixture, which is directly related to its average molecular weight.[17,18] Acoustic sensors have been employed to measure and control the composition of binary inlet gas mixtures in metal-organic chemical vapor deposition processes.[19-21] In this work, we used the Leybold Inficon Composer™ acoustic sensor to detect WF_6 concentration variations in a low molecular-weight gas (H_2) *downstream* of the wafer in a WF_6/H_2 tungsten CVD process. The high mass-ratio between H_2 (2 g/mol) and WF_6 (179 g/mol) results in significant variations of the average molecular weight in the downstream gas mixture from the reactant depletion or product generation occurring on the surface of the wafer and generates a variation of the gas sound velocity.

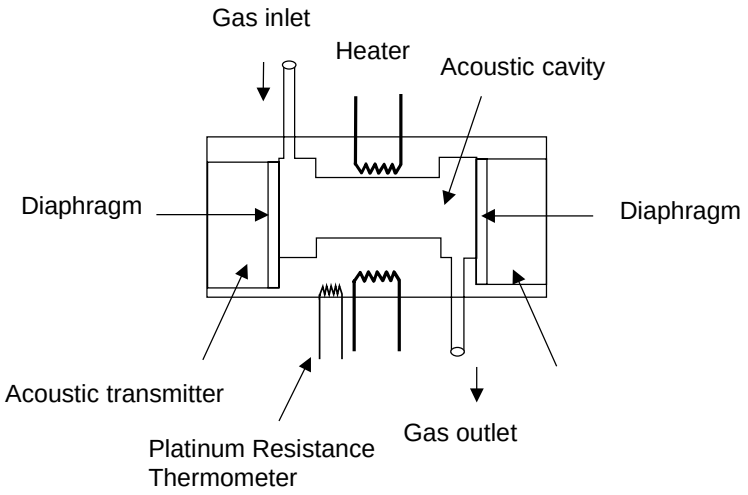

Figure 1: Acoustic sensor schematic. The sound velocity is measured in a Helmholtz resonant cavity that includes two quartz crystals on opposite ends to stimulate and measure the sound intensity. The digitally synthesized frequency is varied via a lock-in amplifier in order to remain in resonance with the gas flowing through the temperature-controlled acoustic cavity.

The sound velocity is measured in a Helmholtz resonant cavity that includes two diaphragms on opposite ends to separate the process gas from the sound generating and detecting means. (Figure 1). The digitally synthesized stimulating frequency is varied via a lock-in amplifier technique in order to remain in resonance with the gas flowing through the chamber. The temperature in the transducers chamber is maintained constant by a precision temperature controlled heating element. The measured sound velocity is function only of the gas composition at a given pressure and is given by the equation below where C, sound velocity, F, frequency, γ_{avg}, average specific heat ratio, T, gas temperature, M_{avg}, average molecular weight, R is the gas constant.

$$C = \sqrt{\frac{\gamma_{avg} \times R \times T}{M_{avg}}} \quad \text{and} \quad F = \frac{C}{2L}$$

EXPERIMENTAL

The W CVD process was performed on a production-scale Ulvac ERA 1000 cluster tool with a water-cooled aluminum chamber and stainless steel exhaust tubing. In the process of this study, W deposition via H_2 reduction of WF_6 was used. Deposition was done on 4" silicon wafers that were heated through a quartz window by a tungsten lamp ring located on top of the reactor. To ensure a constant temperature at the wafer (+/- 10 %) during the process, 6-minute non-constant heat ramps were systematically programmed. The reported process temperatures in this paper are the estimated wafer temperatures, as determined by an instrumented wafer.[22] Prior to deposition, the wafers were cleaned in a 10% aqueous HF solution for 20 minutes, rinsed in deionized water, and blown dry with nitrogen. Cleaned wafers were loaded into the CVD reactor through a high vacuum load-lock. The tungsten deposition rate was measured by ex-situ weight measurement of the wafer.

To sample the process stream, gas was extracted to the Composer at a point immediately downstream of the reactor outlet and upstream of the exhaust throttle valve. Figure 2 shows the configuration of the sampling system. The flow was sampled directly from the pressure controlled reactor at the constant process pressure (0.5 Torr) to maintain a constant pumping speed to the Composer for any given gas composition. The sampled gas was extracted from the reactor at 0.5 Torr and was compressed to at least 50 Torr before entering the acoustic sensor. Pressures above 50 Torr are required in an acoustic sensor so that the gas media density is high enough to carry the energy of the acoustic wave. Such compression from 0.5 to 100 Torr was achieved by sampling the gases through a turbo molecular pump (TMP) backed by a mechanical pump. In addition to the high compression ratio, this sampling setup offered a high gas throughput, for shorter response times from the sensor.

The pumping characteristics for the sampling/compression system were based on a target residence time in the Composer of 1 s with a compression ratio for H_2 of at least 100. Considering an estimated 25 cm^3 low-conductance volume from the outlet of the pumping system to the outlet of the composer (including the acoustic chamber, which has a volume of 18 cm^3), a required 2.5 L.Torr/s throughput was estimated. The gases were sampled through a restrictor at 0.5 Torr so that the estimated pumping speed was at least 5 L/s (25 L/s at 0.1 Torr). In this study a single stage TMP (150 L/s), backed-up by an oil-sealed rotary vane pump (35 L/min) were used. Low vapor pressure PFPE (perfluoro polyether) oil was used in the rotary pump to limit potential reactions that could alter the gas concentrations. The pressure in the sensor was measured downstream by a capacitance manometer and controlled manually by adjusting a metering valve. A mass flow meter was used to monitor the flow through the sensor and the resonant chamber was kept at 60 C to avoid condensation of WF_6.

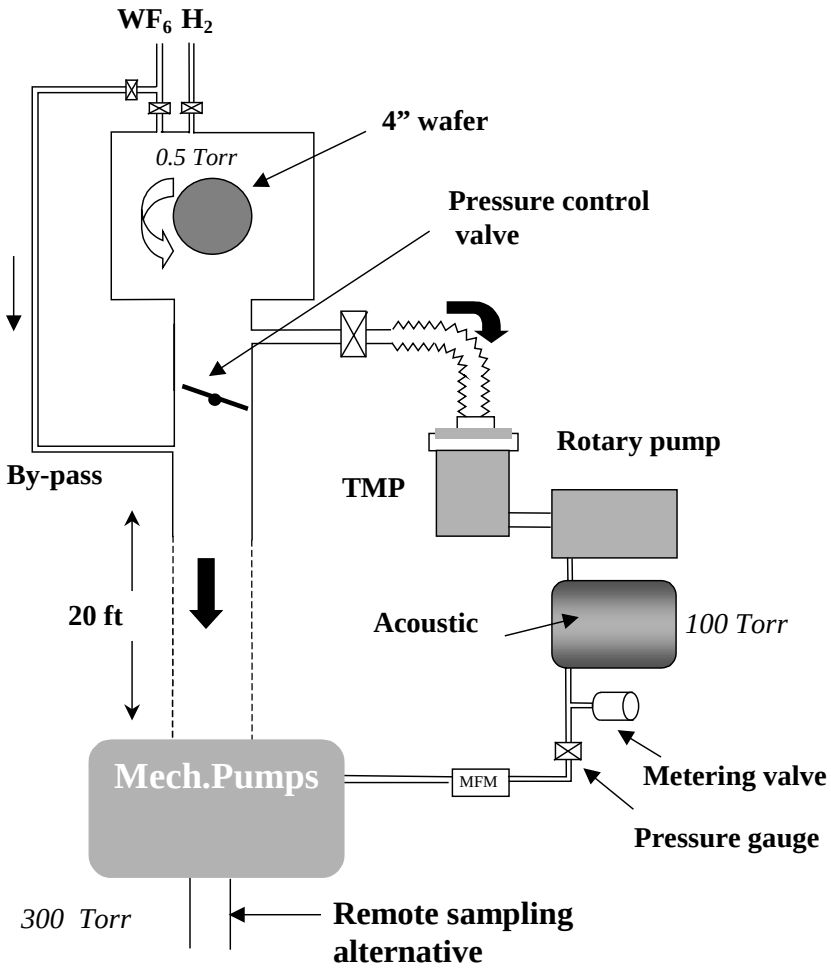

Figure 2: CVD reactor and sampling system. Process gases are sampled into the acoustic transducer from the outlet of the CVD reactor. For acoustic wave propagation, the gases are compressed from 0.5 Torr (process pressure) to 100 Torr through a turbo-molecular pump backed up with a mechanical pump.

In the experiments reported here, Composer data were collected either at fixed flow conditions without wafer heating (i.e., without a deposition reaction) or during a deposition process sequence. A typical tungsten deposition process was done at chamber pressure of 0.5 Torr, nominal substrate temperature of 350 C, and a $[H_2]/[WF_6]$ gas flow ratio of 8 to 1 with 40 sccm H_2. The process sequence in these experiments included the following steps (see figure 5): First, the wafer was loaded and the reactor was flushed with H_2 at 200 sccm. Second, the process gases were flowed through the reactor at 0.5 Torr with the wafer unheated, thus preventing any deposition of WF_6 on the wafer. The signal collected with the wafer unheated provided a baseline for the metrology data and also served to "condition" the walls prior to the reaction. Fourth, the WF_6 flow was by-passed out of the reactor and out of the sensor while the wafer was heated to 350 C during a 5-minute ramp period. Fifth, the WF_6/H_2 process is run for 6 minutes producing approximately 100 nm of tungsten on the wafer. In the final step, 2000 sccm of pure H_2 was flowed to cool down the wafer. During the sequence of steps, the process gases

exiting the reactor was sampled continuously through the acoustic sensor and the pressure in the sensor was controlled at 100 ± 1 Torr using a metering valve. A 5 sccm nitrogen purge was also delivered through the TMP sealing valve and consequently added to the sampled gas mixture.

RESULTS

Sensor response and gas dynamics characterization at room temperature

To characterize the effects of sampling system pumping dynamics on the Composer's response to variations in gas composition in the reactor, data were collected with gas mixtures of H_2 and WF_6 flowing through the reactor at a pressure of 0.5 Torr without a wafer present. Figure 3 shows the temporal variation of the resonant frequency when H_2 flow rates were kept constant at 100 sccm while WF_6 flows were stepped from 0 to 10 sccm (with an additional 12 sccm N_2 purge flow). The time delay between a change in composition (i.e., H_2/WF_6 flow rate) and detection of a frequency variation was approximately 10 s and the time constant for the signal to reach steady state was approximately 100 s. The response delay is a function of the pumping speed. The pump used has a nominal pumping speed of 150 L/s but this decreases significantly above 0.0075 Torr to a value lower by more than an order of magnitude at 0.5 Torr.[23]

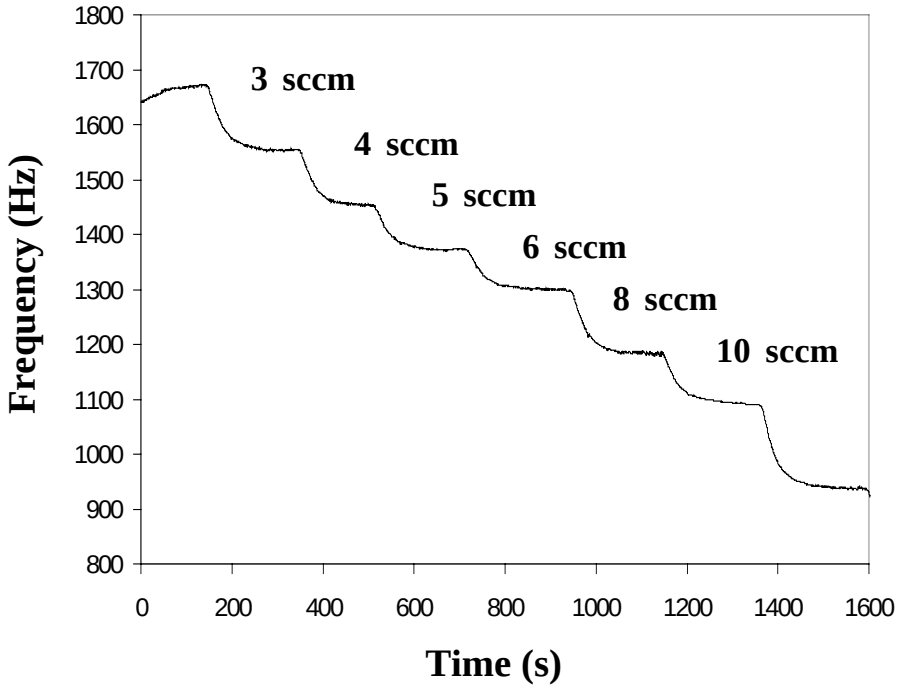

Figure 3: Variation of the resonant frequency with a gas flow of 100 sccm H_2 while WF_6 is stepped from 2 to 10 sccm. A 12 sccm N_2 purge is also added at the TMP sealing flange. No wafer is loaded and the reactor temperature is maintained at room temperature

Figure 4 compares measured sensor data of frequency versus flow composition with theoretical curves of the expected sensor response. The measured data are frequency responses for H_2 flows of 40, 100, and 200 sccm with WF_6 flow rates stepped over time from 0 to 40 sccm. The data points are the steady state frequency for a fixed flow condition such as shown in figure 3. They clearly match the expected non-linearity of the sensor response with a frequency increase when the average molecular weight decreases either by addition of H_2 (2 g/mol) or depletion of WF_6 (179 g/mol). The frequency varies as the inverse of the square root of the average molecular weight as indicated by the good fit of the experimental data (data points in Fig. 4) to the theoretical data based on the acoustic equation (solid lines in Fig. 4). These data suggest that the maximum sensitivity will be reached at higher H_2/WF_6 ratios. For example, at a 40 sccm flow of H_2, sensitivity will increase from 3 to 110 Hz / WF_6 sccm at respectively 1/1 and 10/1 mass ratios. Considering a maximum noise level of ±1 Hz in these conditions, a sensitivity of 50 Hz/WF_6 sccm will ensure a noise/signal ratio below 2% for a 1 sccm variation of WF_6. Such sensitivity is reached for H_2/WF_6 ratios above 4 to 1.

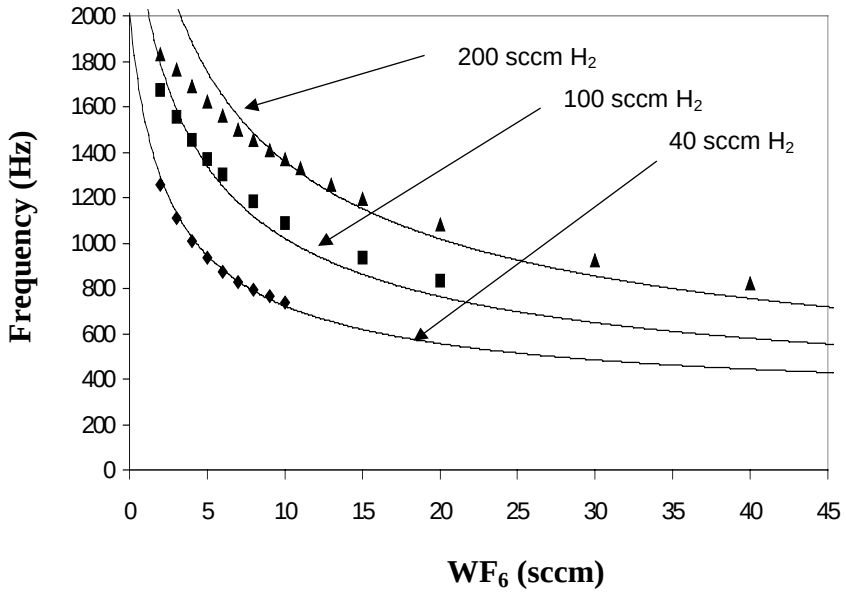

Figure 4: Comparison of measured resonant frequency data with theoretical values based on acoustic model for 3 [H_2/WF_6] gas mixtures at 40, 100 and 200 sccm H_2 flow rates while WF_6 is stepped from 2 to 45 sccm. A 12 sccm N_2 purge is also added at the TMP sealing flange. Inlet gases and CVD reactor are at room temperature and no wafer is loaded.

While the experimental data fits the theoretical values with a less than 2% error in the case at 40 sccm H_2, a significant divergence appears at low WF_6 flow rates with 200 sccm H_2 (and 12 sccm N_2 purge). Indeed the calculated frequency corresponding to 200

sccm H_2 and 12 sccm N_2 is significantly higher (3050Hz – not visible on Fig. 4)) than the estimated frequency from the data (1980Hz). This suggests that the WF_6/H_2 concentration ratio (i.e., average molecular weight) of the gas at the sensor is greater than in the reactor. In this case, the frequency intercept for 0 sccm flow of WF_6 corresponds to a gas mixture containing only 100 sccm of H_2 for 12 sccm of N_2. We believe this effect due to the difference in compression ratios for H_2 and N_2 in the turbo pump and the fact that the process gases are primary exhausted through the mechanical pumps whose compression ratio are relatively mass-independent.

Time-Dependent Sensor Signals through the Process Cycle

The acoustic Composer can detect concentration variation of WF_6 in H_2 as small as 1%. This is sufficient to observe the depletion of WF_6 resulting from the reduction by H_2 during the deposition of W by CVD. For in-situ metrology, the Composer signal was collected during a tungsten deposition process. Figure 5 shows the temporal variation of the resonant frequency during the W CVD process of one wafer. The frequency increased up to 1900 Hz during the flushing, heating ramp and cooling steps in the process cycle are due to the low molecular weight H_2/N_2 flow at those steps. In this experiment the frequency variations during the baseline step (30–390 s) and the process step (630-990 s) were the most important for growth rate metrology purposes. In order to illustrate the frequency difference between these two steps of interest, both signals have been overlaid in figure 6. Frequency signals during both steps stabilized after approximately 3 minutes. The steady state value of the frequency measured during the W deposition is 28 Hz higher than the steady state signal collected under identical flow conditions but with an unheated wafer. Measurement of the higher frequency during deposition indicated a decrease of the average molecular weight due to the relatively lower concentration of WF_6 from the consumption of WF_6 in the tungsten deposition reaction.

In-situ Growth Rate Metrology

To verify the correlation between the reaction rate (i.e., the deposited film thickness) at the wafer and the variation of the acoustic sensor response, 17 wafers were processed following the same recipe at 0.5 Torr, 8 to 1 H_2/WF_6 ratio and a wafer temperature ranging from 300 to 350 C. In order to calculate the frequency variation with an optimal accuracy, the signals from the deposition and conditioning steps were both averaged over the last 60 sec of each step. The relationship between the measured frequency variation and the deposited film thickness is illustrated on figure 7. With a linear regression coefficient R of 0.974 and a standard deviation of 1.49, the relationship appears fairly linear. The error, based on the error to the slope, is 6% while the origin was estimated at (0.08 ± 1.3) Hz.

Figure 5: Resonant frequency variation vs. time during a process cycle at 0.5 Torr, 350 C deposition temperature, 40 sccm H_2 and 5 sccm WF_6. The high frequency values during the heat ramp and the cooling steps result from the absence of WF_6 flow during these steps. The baseline step provides a frequency value reference for the same conditions as the deposition step but with the wafer maintained at room temperature. This baseline accounts for potential frequency drifts resulting primary from chemical interactions of WF_6 on the walls

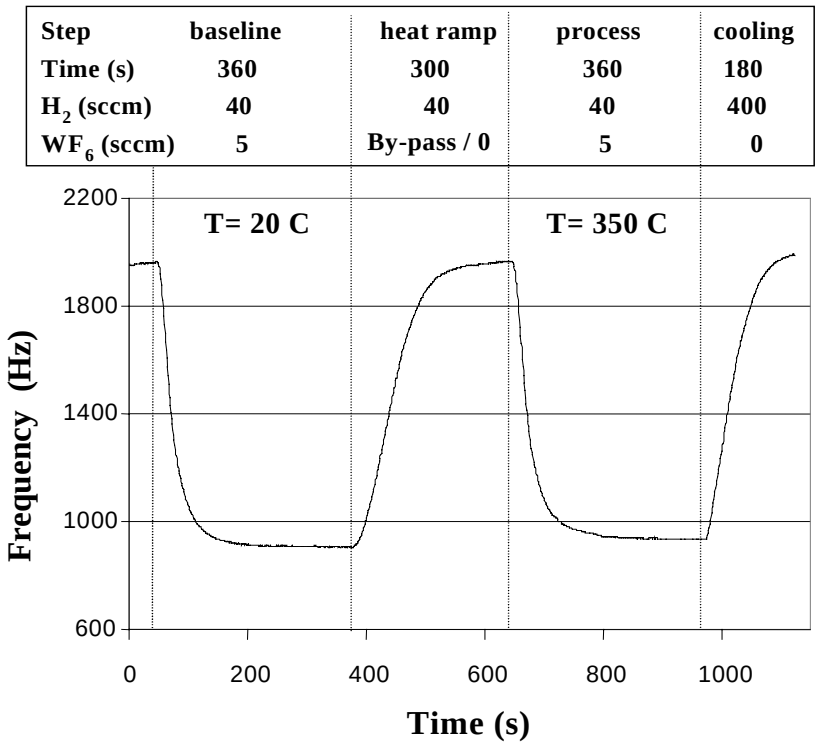

Figure 6: Overlay of the frequency signals during the room temperature baseline step and the 350 C deposition step of the process cycle shown in figure 5. The increase of the frequency, that corresponds to a decrease of the average molecular weight of the sampled gas mixture, results primary from the depletion of WF_6 to deposit a solid tungsten layer. 906.4 Hz and 935.0 Hz are the averaged frequency values over the last 60 data points (1minute) of each step

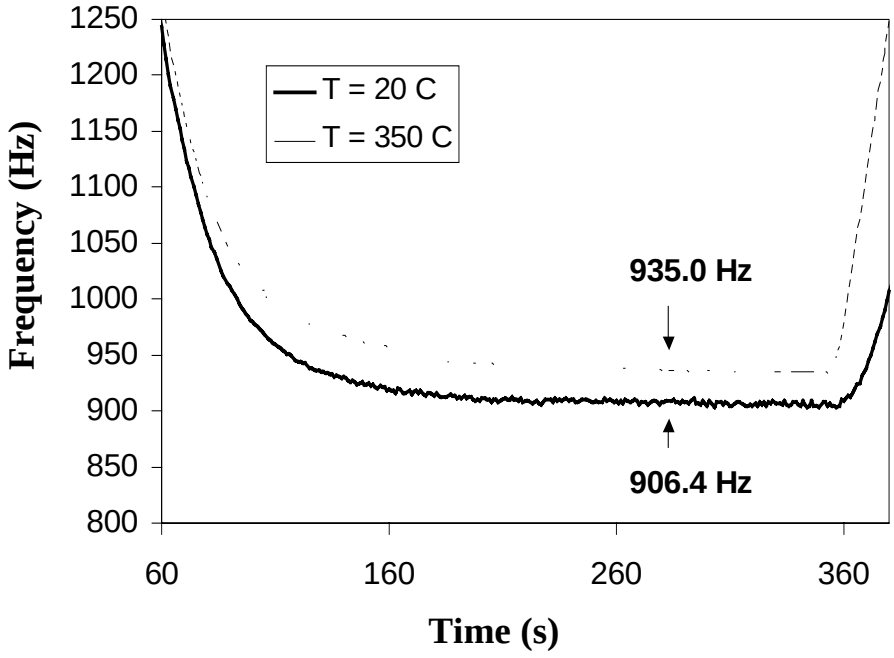

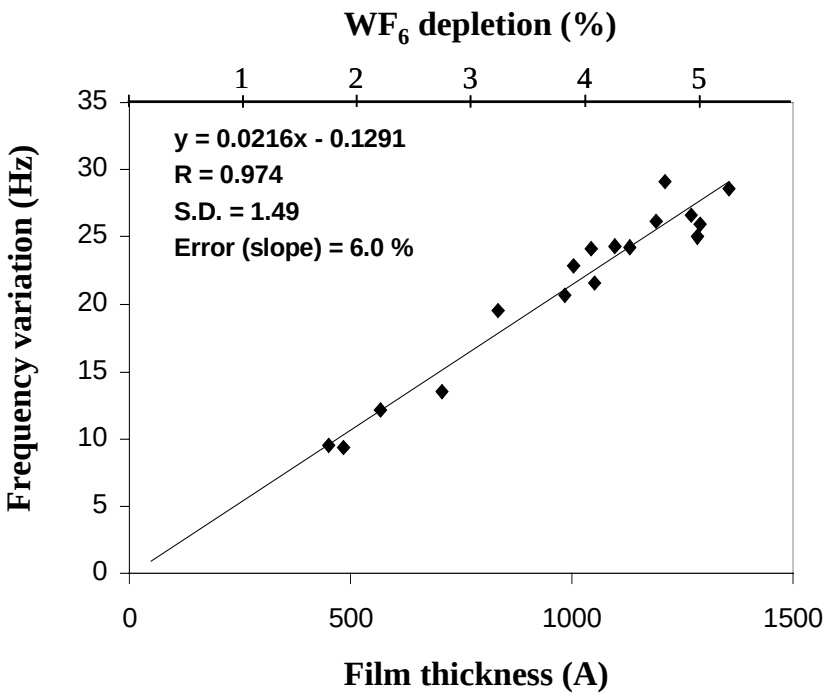

Figure 7: Correlation between the in-situ resonant frequency variation (as shown on figure 6) and the deposited film thickness as determined by ex-situ weight measurements of the wafer. 17 wafers were processed at 0.5 Torr, 40 sccm H_2, 5 sccm WF_6, from 300 to 350C. The precision of the correlation is estimated at 6% based on the error to the slope

DISCUSSION

Acoustic sensor sensitivity and metrology precision

As expected, the WF_6 and H_2 reactant flow provides high molecular weight contrast which elicits sensitivity to reaction on the wafer. The depletion of WF_6 due to film deposition and the resulting decrease of the average molecular weight in the gas phase is detected by the acoustic sensor as a substantial increase of the resonant frequency. Despite the production of HF that would contribute to a partial increase of the mass and consequently affect the sensitivity, WF_6 concentration changes as small as 1% produced a signal variation of over 10 Hz, which is an order of magnitude above the apparatus's noise amplitude. With a precision of the order 6% for this acoustic-based in-situ metrology, the results from the acoustic sensor revealed as good as those reported using sensing approaches such as mass spectrometry.[15] We have demonstrated run-to-run process control of film thickness using mass spectrometry with the thickness and reactant depletion correlated to a similar accuracy.[24] However, to satisfy more stringent metrology requirements as outlined in the international technology roadmap and be capable of maintaining the deposited thickness variations from run to run within a few percent range, it appears critical to target a better accuracy within 1 or 2 percent.

Prognosis for Commercial Processes

Though we previously showed that the acoustic sensor sensitivity is fundamentally a function of the H_2/WF_6 ratio, we expect that the metrology results will be significantly improved at a given ratio for processes with higher depletions that will result in higher frequency variations. The CVD tool used for these experiments was limited to operating pressure of less than 1 Torr producing reaction rates (i.e., WF_6 depletion rates) of approximately 3% or less. Based on our simulation results, a 40% depletion as typically observed on industrial blanket CVD tool would generate a frequency variation of more than 100 Hz, consequently minimizing the error. Such high deposition rates are normally obtained by operating at higher pressure (40 Torr).

Vacuum Technology

Under the conditions studied here, the response delay between a gas composition change (i.e., flow condition) change in the reactor and stabilization of the Composer frequency signal was approximately 100 seconds. This delay is partially a function of the pumping speed. However, we believe reactions and/or adsorption/desorption from internal surfaces of the reactor chamber and exhaust lines are a factor as well. Similar response-time profiles were observed when the same process was analyzed using a differentially-pumped closed-ion source Residual Gas Analyzers (RGA).[15] We believe these dynamic effects are a function of the history of the reactor and are enhanced if the reactor and sampling system walls have not been previously saturated with WF_6 by conditioning the tool. The response time profile is significantly shorter when sampling other gas mixtures such as SF_6/H_2. This chemical dependent behavior suggests that interactions of the WF_6 on the reactor and tubing walls, which is well-known to easily react on the stainless-steel surface (wall effect)[25], contribute to the gas composition detected by the Composer.

Compressing the sampled CVD process flow up to the minimal pressure (50 Torr) for detection by Composer is also a critical issue. We showed evidence that non-constant concentration profiles between the reactor and the sensor environments can result from the mass-selective pumping effects of a TMP at a high intake pressure with gas mixtures rich in H_2. This can be partially addressed by implementing a pump (e.g. a turbo-molecular drag) capable of higher pumping speed (25 L/s) at higher intake pressures. It is worth mentioning that higher H_2/WF_6 flow rate ratio, where these mass-selective effects seemed to be greatest, result in poor conformality in blanket W CVD and are not desirable in manufacturing.[26] Additionally the choice of an adequate compression system in a corrosive environment will be driven by the need to minimize the pump purge flow which dilutes the process gas mixture and diminishes the sensor's sensitivity. Though this effect is minimal when using a TMP whose recommended purge flow is below 15 sccm, it can be a major limitation to the utilization of alternative compression options. For example, preliminary experiments showed that sampling downstream to the process mechanical pumps (roots blower and rotary pumps) though they present a high compression ratio and high throughput, was primary prohibited by the required 1 L/min purge flow to the mechanical pump. Simulation results based on a 5% depletion of WF_6 during process with 40 sccm H_2 and 5 sccm WF_6 showed that while a 15 sccm N_2 purge

would decrease the maximum frequency variation by 17 % (as compared to no purge), a 500 sccm purge would reduce it by 90 %.

Sensor Placement

The location of the downstream sampling is also critical to achieve accurate wafer-state metrology. Sensing remotely from the reactor presents potential advantages such as minimal disturbance of the process and minimizing the footprint in the cleanroom. Our preliminary experience with remote downstream sampling revealed significant challenges with this approach. In experiments sampling downstream at the process pumps using a either a differentially-pumped mass spectrometer or with the acoustic sensor, we observed substantial drifts in the measured gas phase concentrations due to the effects of reactants interacting with the walls of the exhaust plumbing. Indeed WF_6 is readily adsorbed on the stainless steel walls of the exhaust line while slowly desorbing.[25] Consequently reproducibility of the data will become heavily subject to the process history when sampling remotely. These effects may be minimized through exhaust line heating or pre-conditioning of the exhaust lines, although these procedures may not be practical in a manufacturing environment. Another approach is the development of data analysis algorithms to extract the gas-phase composition changes that are purely associated with reactions at the wafer. These and other approaches to in-situ gas-phase chemical sensing are currently being worked on in our group.

Process Recipe

The utilization of a cold wafer sequence used to monitor a reference baseline prior to deposition presents a major limitation in terms of application in manufacturing. This step is presently compulsory since a drift of the order of - 0.2% per run is observed in the sensor frequency response despite up-to 2 hour conditioning periods. Considering that our metrology is based on a frequency signal varying by the order of 1 to 3% (due to our minimal reactant depletion), the error over a few runs would substantially affect the metrology precision. The origins of such drift are in part associated with wall effects due to WF_6 reactivity. Though conditioning helps by saturating the walls with WF_6, minimizing the surface area and heating the walls of the sampling system to 70 C should reduce the conditioning time and limit the consumption of process gases. Additionally the effects of the oil's chemistry are not clear but the oil vapor pressure will be function of the motor temperature and can consequently affect the gas composition (especially if there is a presence of H_2O vapor). The implementation of an oil-free piston pump should be considered for a chemically inert compression alternative.

CONCLUSION

An acoustic sensor measuring the sound velocity of a gas mixture downstream to a WF_6/H_2 tungsten CVD process chamber was used for in-situ wafer-state metrology. Because of the high molecular weight contrast between the reagents, mass-related sound velocity measurements allow the detection of variations of less than 1 % of WF_6 in H_2. This is sufficient to monitor the depletion of WF_6 resulting from the reduction by H_2

despite depletion rates as low as 2 to 5 % in the reactor used in this study. The sensor data were linearly correlated to ex-situ film thickness (based on weight measurements) with an error less than 6% for 17 wafers processed between 300 and 350 C in the sub-torr pressure regime at a 8 to 1 H_2/WF_6 ratio and with 40 sccm of H_2. This is comparable with the accuracy obtained by using mass-spectrometry sensing. Additionally, the expected non-linearity of the sensor response when spanning over a wide H_2/WF_6 ratio range (from 20 to 1) was accurately predicted within a few % error using a simple model based on sound velocity equations for real gases.

This preliminary study showed that the gas compression from 0.5 Torr to above 50 torr for acoustic sensor based monitoring of an LPCVD process could be achieved using a turbo molecular/rotary mechanical pump stack. Issues remain regarding the mass selective pump rates that can generate discrepancies in the composition of the sampled gas mixture as compared to the gas mixture in the reaction chamber. Consequently more adequate compression system, using turbo-drag pump or dry piston pumps, will be investigated in the future.

Reagent and wall reaction, which are well known with WF_6, are also challenging since they are the source of temporal composition drift. In order to compensate for this drift, a baseline had to be monitored prior to deposition in order to be subtracted to acoustic measurements obtained during the deposition step. Also, despite the utilization of synthetic oil for the TMP oil-sealed back-up pump, additional reaction or temperature dependent degas may occur that would aggravate the composition drift. Future work will study the effect of downstream wall heating, wall conditioning and oil chemistry effects. In order to eliminate this time and reactant consuming “baseline” step, we also intend to minimize the relative importance of such drift by increasing the depletion rates of our reactor by an order of magnitude to bring it to the same level as those observed on commercial blanket CVD tools.

Based on these results and with additional improvements of the sampling system, we reasonably expect to increase the accuracy for wafer-state metrology within 1 to 2 %. This would be sufficient for the successful implementation of run-to-run process control. With such metrology capability and the possibility to build simple and accurate models, acoustic sensing may represent a relatively low cost, easy to use, and robust sensor for process applications.

REFERENCES

1 "National Technology Roadmap for Semiconductors 1997," (1998).

2 S. W. Butler, J. Hosch, A. C. Diebold, and B. V. Eck, Future Fab International, issue 2, vol. 1, 315-321 (1997).

3 K.-I. Hanoaka, H. Ohnishi, and K. Tachibana, Jpn. J. Appl. Phys. **32,** 4774-4778 (1993).

4 A. Y. Kovalgin, F. Chabert-Rocabois, M. L. Hitchman, S. H. Shamlian, and S. E. Alexandrov, Journal De Physique **4,** 357-364 (1995).

5 T. K. Whidden and S. Y. Lee, Electrochemical and Solid-State Letters **2,** 527-530 (1999).

6 B. H. Weiller, Material Research Society Proceedings **282,** 605-610 (1993).

7 S. Salim, C.A.Wang, R. D. Driver, and K. F. Jensen, J. Cryst. Growth **169,** 443-449 (1996).

8 J. A. O'Neill, M. L. Passow, and T. J. Cotler, J. Vac. Sci. Technol. A **12,** 839-845 (1994).

9 W. J. DeSisto, E. J. Cukauskas, B. J. Rappoli, J. C. Culbertson, and J. A. Claassen, Chemical Vapor Deposition **5,** 233-236 (1999).

10 W. J. DeSisto, J. Cryst. Growth **191,** 290-293 (1998).

11 B. J. Rappoli and W. J. DeSisto, Appl. Phys. Lett. **68,** 2726-2728 (1996).

12 R. W. Cheek, J. A. Kelber, J. G. Fleming, R. S. Blewer, and R. D. Lujan, J. Electrochem. Soc. **140,** 3588-3590 (1993).

13 L. L. Tedder, G. W. Rubloff, I. Shareef, M. Anderle, D.-H. Kim, and G. N. Parsons, J. Vac. Sci. Technol. B **13,** 1924-1927 (1995).

14 L. L. Tedder, G. W. Rubloff, B. F. Conaghan, and G. N. Parsons, J. Vac. Sci. Technol. A **14,** 267-270 (1996).

15 T. Gougousi, Y. Xu, J. N. Kidder, Jr., G. W. Rubloff, and C. Tilford, J. Vac. Sci. Technol. B **18,** 1352-1363 (2000).

16 M. E. Buckley, Vacuum **44,** 665-668 (1993).

17 C. Gogol, in *R.& D*; *Vol. 41* (1999), p. 29.

18 J. P. Stagg, J. Christer, E. J. Thrush, and J. Crawley, J. Cryst. Growth **120,** 98-102 (1992).

19 S. Yamamoto, K. Nagata, S. Sugai, A. Sengoku, Y. Matsukawa, T. Hattori, and S. Oda, Jpn. J. Appl. Phys. **38,** 4727-4732 (1999).

20 A. Wajid, C. Gogol, C. Hurd, M. Hetzel, A. Spina, R. Lum, M. McDonald, and R. Capik, J. Cryst. Growth **170,** 237-241 (1997).

21 B. R. Butler and J. P. Stagg, J. Cryst. Growth **94,** 481-487 (1989).

22 H.-Y. Chang and R. A. Adomaitis, in *Paper 193c*, Dallas, TX, 2000.

23 *Product and Vacuum Technology Reference Book* (Leybold Vacuum Products Inc, 1995).

24 R. Sreenivasan, T. Gougousi, Y. Xu, J. N. Kidder, Jr., E. Zafiriou, L. Henn-Lecordier, and G. W. Rubloff, to be submitted to Journal of Vacuum Science and Technology B (2000).

25 D. A. Bell, Z. Lu, J. L. Falconer, and C. M. McConica, J. Electrochem. Soc. **141,** 2884-2888 (1994).

26 A. Hasper, J. Holleman, J. Middlehoek, C. R. Kleijn, and C. J. Hoogendoorn, J. Electrochem. Soc. **138,** 1728 (1991).